Physica C: Superconductivity and its applications 606 (2023) 1354212

Contents lists available at ScienceDirect

Physica C: Superconductivity and its applications

journal homepage: www.elsevier.com/locate/physc

Manufacture and performance test result of a 95 kA-class Nb-Ti cable-in-conduit conductor for the low field winding-package of CFETR-TF coil

Chao Dai [a,*], Yu Wu [a], Kamil Sedlak [c], Hugo Bajas [c], Arend Nijhuis [b], Pierluigi Bruzzone [c], Arnaud Devred [e], Jinggang Qin [a], Yunhao Liu [d], Tianjun Xue [f], Zuojiafeng Wu [g]

[a] *Institute of Plasma Physics, Chinese Academy of Sciences, Hefei 230031, China*
[b] *University of Twente, Energy, Materials and Systems, Faculty of Science and Technology, Enschede 7500AE, the Netherlands*
[c] *École Polytechnique Fédérale de Lausanne (EPFL), Swiss Plasma Center (SPC), 5232 Villigen-PSI, Switzerland*
[d] *University of Science and Technology of China, Hefei 230026, China*
[e] *CERN, TE Department, Geneva 23 1211, Switzerland*
[f] *Baiyin Non-ferrous Changtong Wire & Cable Co. Ltd., Baiyin, Gansu 730900, China*
[g] *Longteng Mechanical and Electrical Co. Ltd., YiChun 336000, China*

A R T I C L E I N F O

Keywords:
CFETR TF
Cable-in-conduit conductor
Nb-Ti conductor

A B S T R A C T

The engineering design of the CFETR TF prototype coil and conductors has been completed. The wind-package (WP) of the coil is graded into three regions based on the magnetic field distribution for saving cost. High-J_c Nb_3Sn strand, ITER-like Nb_3Sn strand and Nb-Ti strand are applied for high-field, mid-field and low-field WP respectively. In order to verify the conductor design, full-size short samples have been manufactured for the three types of conductors. The samples are tested in the SULTAN facility at CRPP in Villigen, Switzerland. At present, the test of Nb-Ti conductor for low-field WP is finished, DC and AC tests were performed. In DC test, several current sharing temperature (T_{cs}) measurements were performed with 500 electromagnetic cycles and one thermal cycle. Additionally, minimum quench energy (*MQE*) measurement was performed for investigating the stability of the conductor. The test results and analysis are reported in this paper.

1. Introduction

The Comprehensive Research Facility for Fusion Technology (CRAFT) is one of the Chinese national big science and technology facilities. Its mission is developing key technologies and key prototype systems for fusion.

The Toroidal field (TF) coil is one of the most challenging components in the manufacture of the future Chinese Fusion Engineering Testing Reactor (CFETR). Thus, in the CRAFT project, a full-size prototype CFETR TF coil will be built, for developing and verifying the significant technologies such as the superconducting material, Cable-in-Conduit Conductor (CICC) design and manufacture, coil winding package (WP) and coil case manufacture.

According to the CFETR engineering design, the major and minor radii of the CFETR are $R = 7.2$ m and $a = 2.2$ m respectively, with the Toroidal field $B_t = 6.5\ T\ @\ R = 7.2\ m$. The peak field of the TF coil WP is 14.4 T. In order to reduce the cost, the WP is graded into three regions, based on the magnetic field distribution on the inboard leg cross-section, which are high-field (HF) sub-WP, middle-field (MF) sub-WP and low-field (LF) sub-WP (shown in Fig. 1). The main parameters of CFETR TF coil are listed in Table 1.

High-J_c Nb_3Sn strand, ITER-like Nb_3Sn strand and Nb-Ti strand are applied for HF sub-WP conductor, MF sub-WP conductor and LF sub-WP conductor respectively. In order to reduce the difficulty of manufacturing, the geometric dimensions and cable layout of the three types of conductors are identical.

For verifying the design parameters and manufacturing process of the three types of conductors, three pairs of short conductor samples have been manufactured. The performance test of the Nb-Ti conductor for LF sub-WP has been done in the SULTAN facility at SPC, Switzerland, 2021. The manufacturing process of the short conductor sample and test results will be presented in this paper.

* Corresponding author.
E-mail address: dc@ipp.ac.cn (C. Dai).

https://doi.org/10.1016/j.physc.2023.1354212
Received 13 April 2022; Received in revised form 25 November 2022; Accepted 20 January 2023
Available online 26 January 2023

2. Conductor specification and manufacture

According to the conductor design criterion, the minimum temperature margin is required to be 1.2 K, i.e., the current sharing temperature of the conductor shall be: $T_{cs} > 5.7\ K$ @ $5.5\ T,\ 95.6\ kA$.

The geometry of the CFETR TF conductor is circle-in-square, which is similar as the ITER PF and CS conductor, the cross-section of the conductor is shown in Fig. 2 and the main parameters of the conductor are listed in Table 2.

The cable of CFETR TF conductor is a five-stage cable, which consists of six petals and one central cooling spiral. In each petal, there is a segregated copper core in the form of a 2nd stage cable, for increasing the cross-sectional area of copper. Differently from the Nb_3Sn cables of the HF sub-WP and MF sub-WP conductors, which contain a short twist pitch configuration to prevent irreversible performance degradation due to strand movement within the cable, a regular ITER Nb-Ti-type twist pitch configuration was applied to this Nb-Ti conductor. Petal wraps are applied for reducing the coupling loss. The final diameter of the cable is compacted to 49.0 mm, which leaves a gap of 3 mm in conduit diameter for cable insertion before jacket compaction. The main parameters of the cable are list in Table 3.

The Nb-Ti strand for the CFETR TF LF sub-WP conductor is developed by Western Superconducting Technologies Co, Ltd (WST), the technical specifications of the strand are listed in Table 4. This type of strand is intended to be used for the final TF conductor manufacture.

3. Test description

3.1. Sample preparation

The test sample for the SULTAN facility consists of two conductor legs, which are made into U-shape and inserted from a vertical test well into the high field region of SULTAN background magnet [2]. The Nb-Ti SULTAN sample can be made of one conductor length and bent to a U-shape at the bottom [3]. However, the cable diameter of the CFETR TF conductor is too large for make a U-shape bend at the bottom within the available space, thus the 'solder filled' joint technology was adopted as it was used in the ITER Nb_3Sn conductor and MBCN4 Nb-Ti conductor sample tests [3, 4].

Also due to the large diameter of the conductors and cables, two other issues were encountered during sample preparation. First, the overall conductor dimension is too large for the SULTAN test well (142 × 92 ± 0.5 mm) and then there is no space for clamps and sensors installation. The solution is milling part of the conduit section of the conductor, as shown in Fig. 4. Second, the cable diameter is too large for both upper and lower terminations since the distance of the clamps of the superconducting transformer is 100 mm. For reducing the cable diameter, the cable was disassembled at the ends and part of the copper wires were removed, reducing the cable diameter from 47.6 to 43.0 mm. Then the cabling pattern was re-established manually, and cable terminations were inserted into copper sleeves. The process is shown in Fig. 3.

The instrumentation arrangement of the sample is similar to previous Sultan samples, mainly including voltage taps and temperature sensors. The only difference is that the number of temperature sensors upstream and downstream of the high-field region is reduced to three, compared to four sensors in a typical sample due to space limitation, as illustrated in Fig. 4.

Table 1
The main parameters of the CFETR TF coil.

Parameter	Unit	value
Number of TF coils	–	16
Operating current	kA	95.6
Peak field	T	14.4/10.6/5.5
Operating temperature	K	4.5
Number of turns	–	154
Stored energy per TF coil	GJ	7.5
Weight of one TF coil assembly	ton	750

3.2. Test procedure

The main aim of the test is to determine the T_{cs} and I_c evolution of the conductor under cyclic electro-magnetic (EM) load and warm-up-cool-down (WUCD), in order to verify whether or not the conductor meets the requirements on performance stability. Normally, the test condition should be similar to that of its operation condition, i.e., 5.5 T x 95.6 kA for the CFETR TF LFWP conductor. However, it is experimentally much easier and less time consuming to perform the EM cycles with decreased current and increased background magnetic field, as 7.13 T x 73.7 kA (here 7.13 T consists of the SULTAN background field, 6.0 T, plus the peak self-field of the sample, 1.13 T), which provides load equivalent to the operation condition.

Measuring the T_{cs} at the operation condition 5.5 T x 95.6 kA was attempted at the initial stage with several trials to ramp the current up to 95.6 kA at zero background field, but this failed at around 90 kA. The limitation seems to originate in the secondary winding of the SULTAN superconducting transformer. The attempts to rise current up to 95.6 kA ended up by premature current switch-offs, with sudden voltage take off without any trace of current-sharing and without any temperature rise

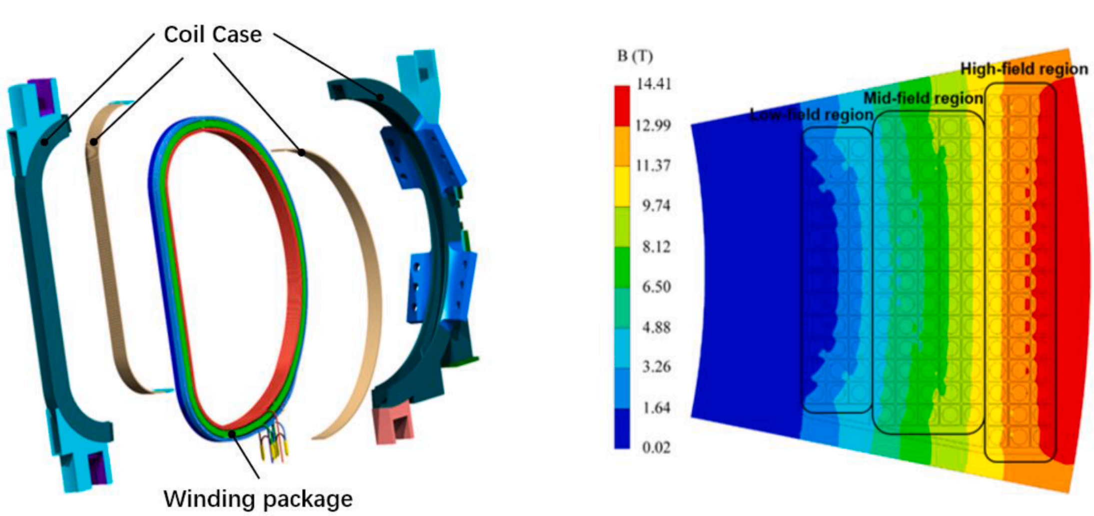

Fig. 1. The profile of the CFETR TF coil (left), and the magnetic field distribution in the inboard leg cross-section (right).

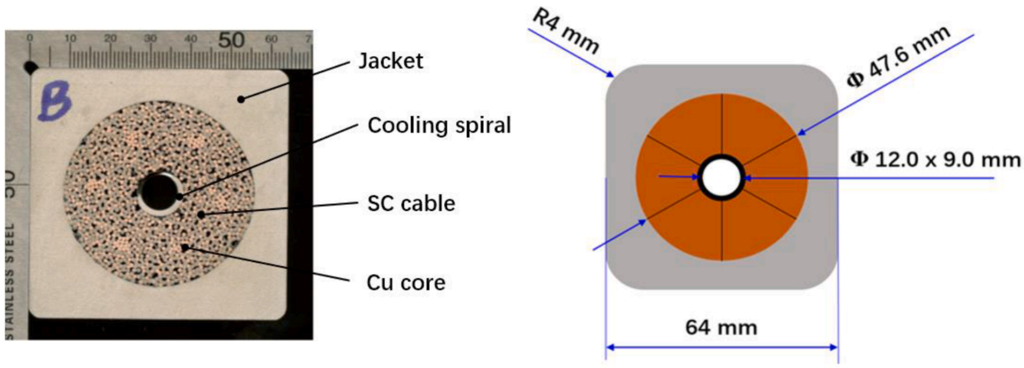

Fig. 2. Cross-section of the conductor cut by electro-erosion (left) and the dimensions of the conductor (right).

Table 2
Main parameters of the CFETR TF LF sub-WP Nb-Ti conductor.

Parameter	Value
Strand type	Nb-Ti
Ni coated strand diameter	0.99 mm +0/−0.005 mm
Number of sc strands	900
Number of Cu strands	522
Conductor outer dimension	64 × 64 mm ± 0.2 mm
Cable diameter	47.6 mm
Central spiral	Φ12.0 × 9.0 mm ± 0.2 mm
Void fraction (bundle area)	~30%
Jacket material	316 LN

Table 3
Main cable parameters of the Nb-Ti conductor.

Cable pattern	((2 sc + 1 Cu) x 3 × 5 × 5 + core) x 6
Copper core pattern	(3 × 4 Cu)
Twist direction	Right hand
Cable twist pitches	
- stage 1 (2 sc + 1 Cu)	80 ± 5 mm
- stage 2 (x 3)	140 ± 10 mm
- stage 3 (x 5)	190 ± 10 mm
- stage 4 (x 5 + core)	300 ± 15 mm
- stage 5	420 ± 20 mm
Core twist pitches	
- stage 1 (3 Cu)	80 ± 5 mm
- stage 2 (x 4)	140 ± 10 mm
Wrapping direction	Left hand
Petal wrap	0.05 mm thick, 20 mm width, 50% cover
Cable wrap	0.10 mm thick, 40 mm width, 40% overlap
Cable diameter (before compaction)	49.0 mm

Table 4
The specification of the Nb-Ti strand for the TF LFWP conductor.

Parameter	Value
Ni-plated strand diameter	0.99±0.005 mm
Filament diameter, D_f	≤11 μm
Inter-filament spacing, S_f	≥1 μm
Twist pitch	15 ± 2 mm
Twist direction	right hand twist
Ni plating thickness	2 + 0/−1 μm
Un-reacted, Ni-plated strand Cu-to-non-Cu volume ratio	1.6 (−0.05/+0.15)
Residual Resistivity Ratio of Ni-plated strand (between 273 and 10 K)	>100
Minimum critical current at 4.22 K and 6.4 T (as measured on ITER barrel)	550 A
Resistive transition index at 4.22 K (n-index) (as measured on ITER barrel)	> 20 (0.1 to 1 μV/cm)
Maximum hysteresis loss per strand unit volume at 4.22 K over $a \pm 1.5$ T cycle	<100 mJ/cm^3

anywhere in the sample after the switch off. The latter is a strong indication that no quench has been initiate in the sample, and it very likely started in the secondary winding of the transformer. Due to this issue, the final T_{cs} test is performed at 7.13 T x 73.7 kA. In addition, the current in AC loss and *MQE* tests was decreased from 90 to 70 kA. The test campaign was generally carried out using the following main steps:

(1) Calibration runs for instrumentation;
(2) AC loss tests before EM cyclic loading;
(3) Reference dc tests before EM cyclic loading;
(4) EM cyclic loading (500 cycles, T_{cs} at cycle #50, #250, #400+WUCD, #500);
(5) AC loss tests after EM cyclic loading;
(6) Minimum quench energy (*MQE*) tests after EM cyclic loading.

4. Experimental results and analysis

4.1. Quench and effect of EM cycles

In previous Nb-Ti conductor tests in SULTAN, two kinds of behaviors of the superconductive-to-normal transition of the conductor could be observed [3]. At low current densities and high applied magnetic fields, a ‘smooth transition’ can be observed, i.e., the voltage signal varies exponentially and exceeds the voltage criterion for critical current. At high currents and low magnetic fields, generally a ‘fast transition’ is observed (shown in Fig. 5). This is physically related to the development of a quench in the conductor, and its corresponding transition temperature is generally referred to as T_q. In this conductor sample test, no T_{cs} was measured, and only a quench T_q was observed. The T_q evolution with EM cycles is shown in Fig. 6 and no change in performance is observed, except perhaps a slight increase in T_q after WUCD. This means that EM cyclic loading does not significantly impact the performance, just as it was the case with previous ITER Nb-Ti conductors.

4.2. Strand performance vs. conductor performance

For assessing the conductor performance, the critical surface $J_c(B, T)$ and transition index $n(J_c)$ of the Nb-Ti strand is required. The critical currents of the Nb-Ti strand at various temperatures and magnetic fields were measured at the University of Twente, and the test data are fitted by the scaling law in [1]. Fig. 7 shows the measured data and fitted curves at various temperatures and magnetic fields. The fitting parameters are listed in Table 5. Fig. 8 shows the n-index as a 3rd order polynomial function of the critical current density.

In order to compare the performance of the tested conductor to that of its constituting strands, a numerical method is applied. First, the magnetic flux density in the conductor cross-section was meshed and discretized, then a magnetic flux density map was obtained. Here the

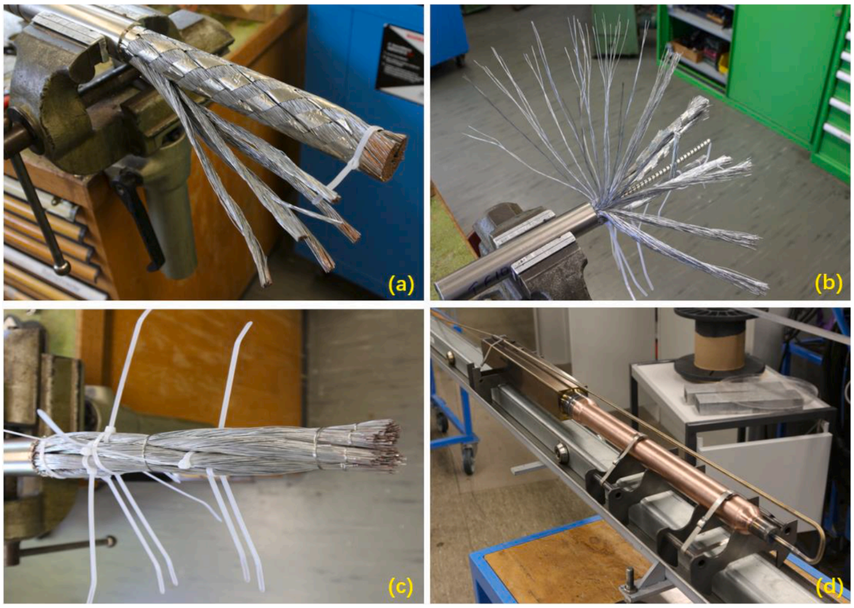

Fig. 3. (a) The steel jacket in the termination region is removed and the cable sub-bundle is dismounted. (b) The central copper wires are removed from each cable petal. In addition, the cable is disassembled to the level of triplets, and additional copper wires from some triplets are removed. In total 300 copper wires are removed. The removed strands are equally distributed through the cable cross section (i.e. from all petals, as well as within each petal). (c) After the removal of the copper wires, the cable geometry is re-established manually as good as possible. (d) The cable termination is inserted into a copper sleeve and crimped to a reduced diameter.

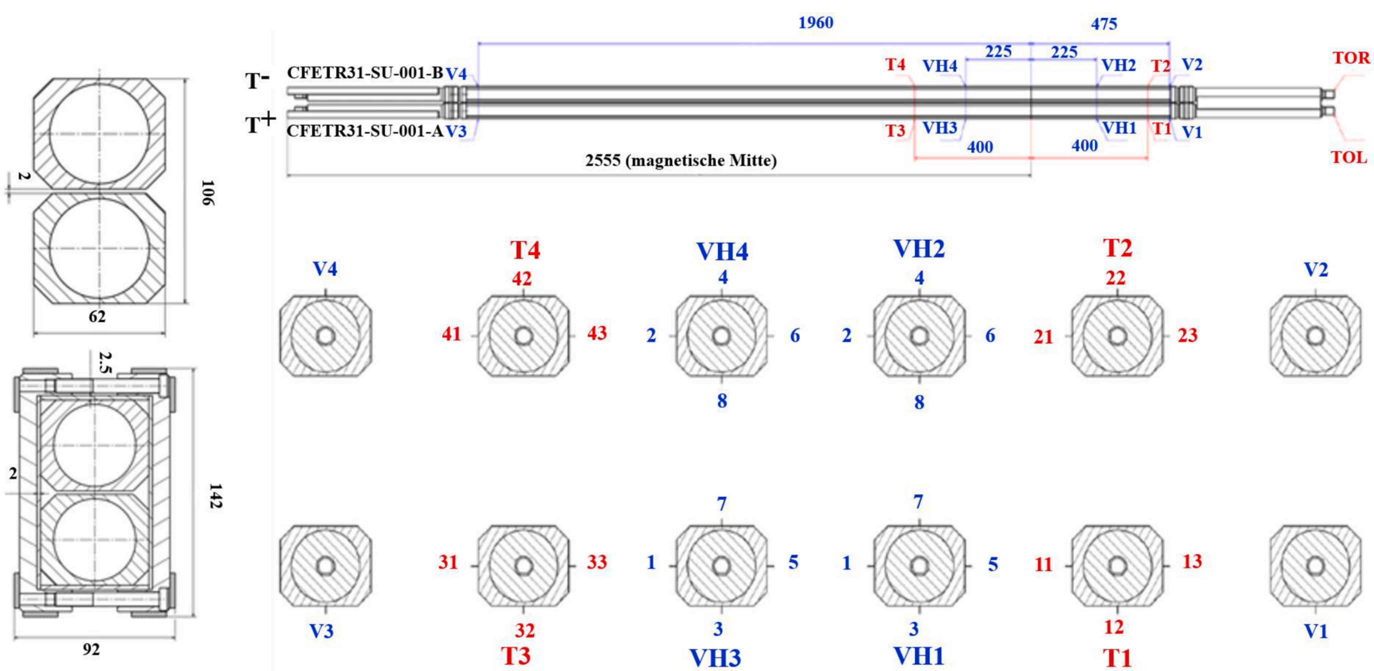

Fig. 4. Sketch of the SULTAN sample with upper terminations, bottom joint, temperature sensors and voltage taps. The dimensions of the conductor cross section after milling are shown at the bottom.

magnetic flux density distribution in the longitudinal direction was considered to be uniform. Then the cable characteristics can be calculated with the strand scaling parameters and the magnetic flux density map over a selected range of temperature, by Eq. (1).

$$E = \frac{E_c}{A_{sc}} \int \left(\frac{J}{J_c(B,T)} \right)^{n(J_c)} dA \tag{1}$$

Where $n(J_c) = -2.0492e^{-11} J_c^3 - 4.6824e^{-6} J_c^2 + 0.027537 J_c + 3.7091$, and $J_c(B,T)$ is the scaling relationship found for the Nb-Ti strand.

The calculated *E-T* is shown in Fig. 9 (solid line), the value of the calculated conductor T_{cs} is then determined as the temperature at which the electric field E reaches the critical value E_c, conventionally set to 10 μV/m. The calculated T_{cs} is 5.69 K, which means the conductor performance agrees well with that of strand performance. Based on the conductor test results, it can be extrapolated that the T_{cs} of the conductor at 95.6 kA x 5.5 T is 6.3 K (dash line), which satisfies the conductor technical specification, $T_{cs} > 5.7\ K$.

4.3. AC loss results

The AC loss tests were performed before and after the DC tests, for evaluating the effect of the EM and thermal cyclic loading on the AC behavior of the cables. The AC loss tests ran at 2 T and 5.5 T SULTAN background field without transport current, and 5.5 T with 70 kA

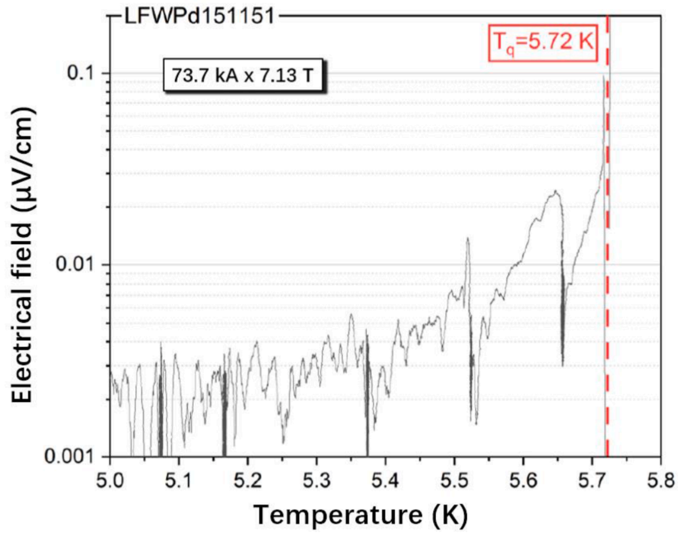

Fig. 5. The *E-T* trace of one of the T_{cs} runs showing that the sample quenches before the electrical field reaches the E_c criterion.

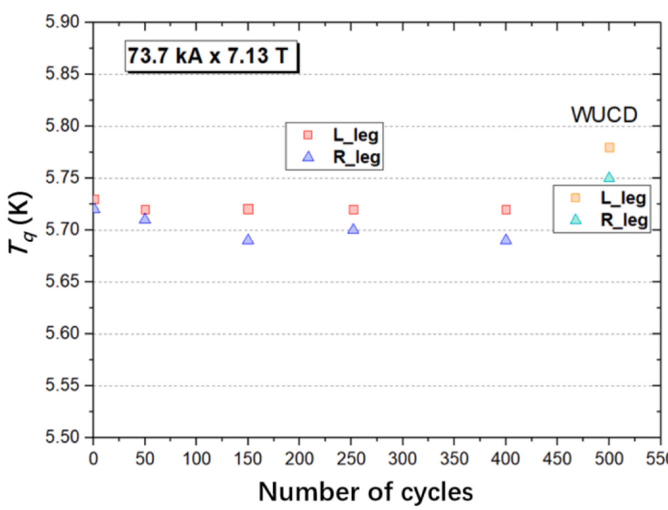

Fig. 6. The T_q evolution with EM cycles and WUCD.

transport current.

In AC loss measurement, the AC loss in the conductor sample is excited by a saddle shaped AC coil, which can generate a pulsed field transverse to the sample axis [9]. The energy from AC loss is measured with a steady state gas flow calorimetric method. The energy deposited into the helium causes the helium temperature and pressure variation, which is sensed by the sensors upstream and downstream. Then the energy can be calculated as:

$$E = \int \frac{dm}{dt} (H(P, T_D) - H(P, T_U)) dt. \quad (2)$$

Where H is the enthalpy of the helium, dm/dt is the helium mass flow rate, and T_U, T_D are the average upstream and downstream temperature respectively. The detailed data processing method can be found in [5].

Table 5
The critical current fitting parameters of the Nb-Ti strand.

(A/T/mm^2)	B_{C20} (T)	T_{c0} (K)	α	β	γ
148,000	14.2	9.12	1.05	1.41	2.13

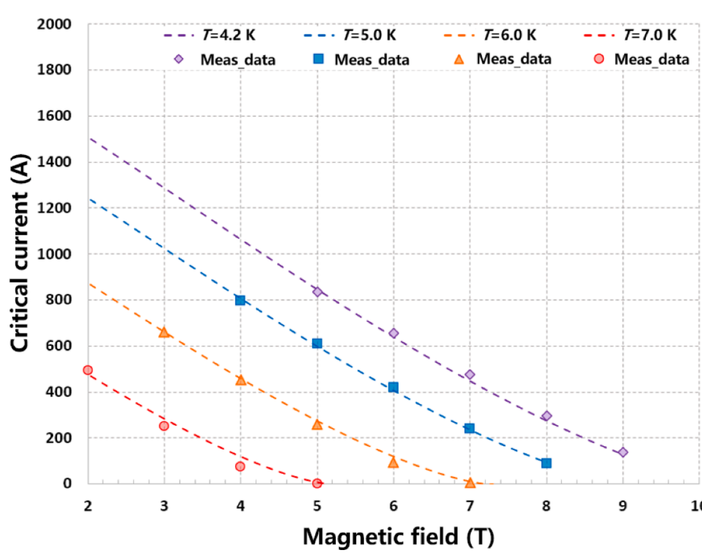

Fig. 7. The Nb-Ti strand critical current as function of *B* and *T*.

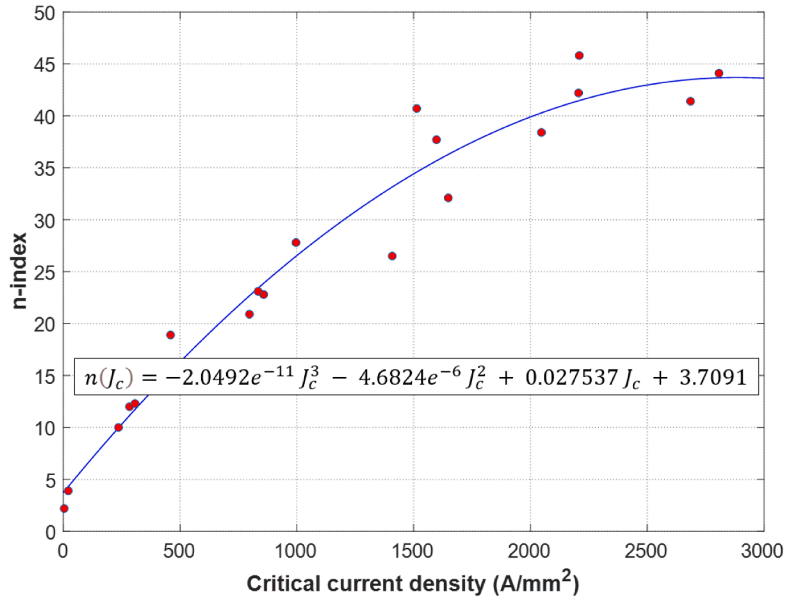

Fig. 8. The *n*-index as a function of critical current density.

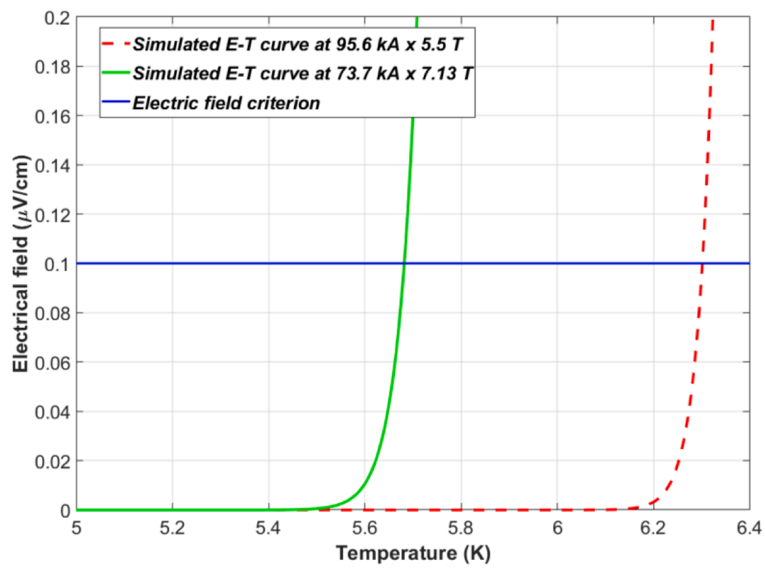

Fig. 9. The simulated *E-T* curves, the solid line is the *E-T* curve under test condition and the dash line is the *E-T* curve under the conductor operating condition.

The AC loss test results are shown in Fig. 10. The results indicate that the cyclic loading has no significant impact on the AC loss. The same observation was reported for the ITER Nb-Ti conductors. On the contrary, the cyclic loading has great impact on the AC loss for Nb_3Sn conductor, because the strands in Nb_3Sn conductor are sintered after heat-treatment and inter-strand contact resistance is significantly reduced before EM cycling. The AC loss reduces when the magnetic field is increased, this is mainly due to the magnetoresistance of the copper matrix [6].

The coupling loss time constants $n\tau$ of the sample are calculated with the relation [7]:

$$n\tau = \alpha \frac{\mu_0}{2\pi^2 B_a^2}$$

where B_a is the amplitude of the field ramp and α is the slope of the loss–frequency dependence curve in low frequency region. The time constants and the hysteresis loss Q_{hys} of the sample are listed in Table 6.

4.4. MQE results

The *MQE* tests were performed after the DC and AC tests, to assess the minimum quench energy of the conductor. The test condition is similar to that of the DC test, i.e., at 7.13 T x 73.7 kA. The tests are performed by injecting power with the SULTAN AC coils, as done during the AC loss test. The amplitude of the AC magnetic field pulse is increased step by step until a quench occurs in the conductor.

Similar as for the AC loss test, the calorimetric method is applied to measure the energy deposition. Before the sample quenched, the energy induced by each external field pulse can be computed. When the sample quenched, the temperature increased rapidly and it is not possible to distinguish whether the energy comes from the ac pulse or ohmic heat. Thus, the deposited energy which induces the quench can be calculated by linearly extrapolating the last two data points before the quench. The *MQE* value is defined as the average between the extrapolated quench energy and the maximal deposited energy which allows recovery. [3, 8].

Fig. 11 shows the *MQE* of this conductor sample as a function of its

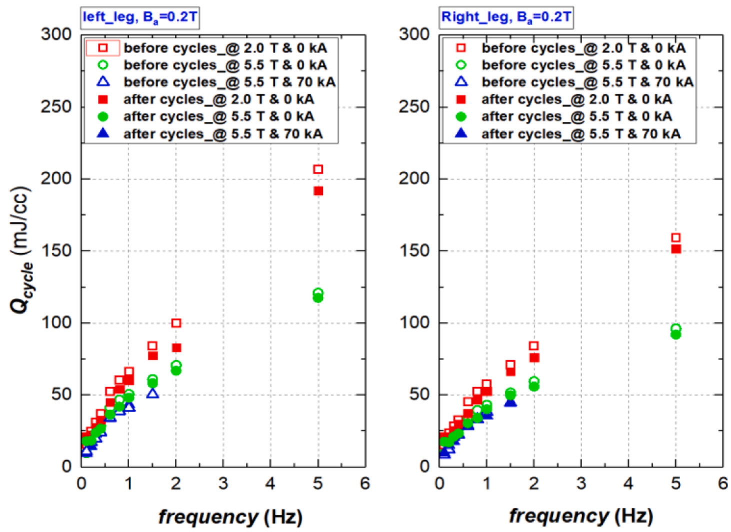

Fig. 10. The AC loss of the sample at different test conditions before and after EM cyclic loading.

Table 6
AC coupling loss time constants and hysteresis loss values of the sample at various conditions.

	Left leg				Right leg			
	2.0 T virgin	5.5 T	2.0 T cycled	5.5 T	2.0 T virgin	5.5 T	2.0 T cycled	5.5 T
$n\tau$ (ms)	101	73	60	48	93	81	90	51
Q_h (mJ/cc)	14	15	10	12	11	10	9.5	11.5

temperature margin between the operating temperature at which the *MQE* measurement was performed and the measured T_q at the same test condition. Also, the *MQEs* of this conductor sample is compared with that of ITER Nb-Ti conductors.

As shown in the plot, the *MQE* increases with the temperature margin, as expected. The *MQE* of the CFTF-Nb-Ti sample is relatively low compared to the ITER conductors (The main parameters of the conductors in comparison are listed in Table 7). The difference should be attributed to the different thermo-hydraulic parameters of the conductors. Among them, void fraction should be a major factor, because void fraction impacts the heat transfer between strands and helium, compared with ITER Nb-Ti conductors, the void fraction of CFTF-NbTi conductor is relatively low. The second possible reason is the self-field gradient is large of this conductor sample, which reduces the stability of the Nb-Ti conductor. the Although the temperature margin of the conductor under operation condition is higher than that under test condition, this issue still needs to be carefully considered when analyzing the transient heat load on the conductor during operation in the future, such as the disturbance at the moment of plasma disruption.

5. Conclusion

In order to verify the design of the Nb-Ti conductor for the low field winding package of the CFERT-TF prototype coil, a sample was manufactured and tested in the SULTAN test facility.

The DC test results show that the conductor is able to sustain the EM load equal to its operation condition and the performance of the conductor is stable after 500 EM cycles and one warm-up cool-down cycle. The TF conductor performance agrees well with the single strand performance and meets the requirements.

The AC loss tests show that the impact of EM cyclic loading on the

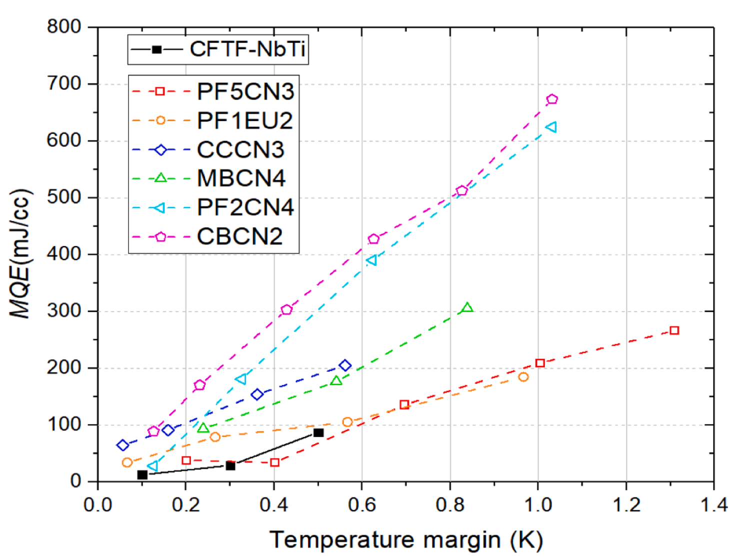

Fig. 11. Minimum quench energy of the CFTF-Nb-Ti conductor as a function of the temperature margin, the results are compared with the results of ITER Nb-Ti conductors in [3].

Table 7
The main parameters of ITER Nb-Ti conductors in [3].

Parameter Conductor shape	PF1EU2 Circle-in-Square	PF2CN4	PF5CN3	CCCN3 Square	MBCN4 Circular	CBCN2
Conductor dimension (mm)	53.8 × 53.8	51.9 × 51.9	51.9 × 51.9	19.2 × 19.2	44.5	22.0
Cable diameter (mm)	37.7	35.3	35.3	14.8 × 14.8	40.5	18.0
Central spiral inner diameter (mm)	10	10	10	n.a.	n.a.	5.0
Cable layout	3sc × 4 × 4 × 5 × 6	(((2 sc+1 Cu strand) × 3 × 4 + 1 Cu core 1) × 5)+1 Cu core 2	(3sc × 4 × 4 × 4)+1Cu core 3	3sc × 4 × 5 × 5	(2 sc+1Cu) × 3 × 5 × (5 + 1C0) × (6 + 1 C1) C0: 3 × 4Cu C1:1 + 6 + 12+18+24	(2 sc+1Cu) × 3 × 3 × 3 × 4
Void Fraction (%) (bundle region)	34.3	34.2	34.1	35.4	32	35

conductor AC loss is very limited.

The minimum quench energy test was performed at DC test conditions and various temperatures. The test results showed that the *MQE* increases with the temperature margin, and is relatively low compared with ITER Nb-Ti conductors, which indicates that the impact of the energy disturbance on the TF coil operation must be carefully considered.

Declaration of Competing Interest

The authors declare that they have no known competing financial interests or personal relationships that could have appeared to influence the work reported in this paper.

Data availability

No data was used for the research described in the article.

References

[1] L. Bottura, A practical fit for the critical surface of Nb-Ti, IEEE Trans. Appl. Superconduct. 10 (1) (2000) 1054–1057.
[2] P. Bruzzone, M. Bagnasco, M. Calvi, Test results of two European ITER TF conductor samples in SULTAN, IEEE Trans. Appl. Superconduct. 18 (2) (Jun, 2008) 1088–1091.
[3] M. Breschi, D. Carati, D. Bessette, Performance analysis of the Nb−Ti conductor qualification samples for the ITER project, Superconduct. Sci. Tech. 28 (11) (2015), 115001.
[4] M. Breschi, D. Macioce, A. Devred, Performance analysis of the toroidal field ITER production conductors, Superconduct. Sci. Tech. 30 (5) (2017), 055007.
[5] D. Bessette, M. Breschi, C. Calzolaio, Sensitivity analysis of Tcs measurement on ITER TF conductors, IEEE Trans. Appl. Superconduct. 20 (3) (2010) 1488–1491.
[6] Y. Shi, F. Liu, H.J. Liu, Coupling Loss Characteristics of Nb_3Sn CIC Conductor for CFETR CS Model Coil, IEEE Trans. Appl. Superconduct. 27 (8) (Dec, 2017).
[7] K. Yagotintsev, W.A.J. Wessel, A. Vostner, Overview of verification tests on AC loss, contact resistance and mechanical properties of ITER conductors with transverse loading up to 30000 cycles, Superconduct. Sci. Tech. 32 (10) (2019), 105015, 2019/09/13.
[8] C. Dai, Y. Wu, J. Li, Stability analysis on Nb_3Sn sample conductor of CFETR central solenoid model coil, Fus. Eng. Des. 133 (2018) 59–63, 2018/08/01/.
[9] P. Bruzzone, A. Anghel, A. Fuchs, et al., Upgrade of operating range for SULTAN test facility, IEEE Trans. Appl. Superconduct. 12 (1) (Mar, 2002) 520–523.